BL-3A/2023G509

Modulating magnetic anisotropy in square-lattice pseudo-spin-half systems

Enyang Men[1,2], Deyang Li[1,2],Zhihan Qiao[1,2], Haiyang Zhang[1,2], Hangtian Wang[1,2], Hironori Nakao[3], Lin Hao[1,*]

[1]*Anhui Provincial Key Laboratory of Low-Energy Quantum Materials and Devices, High Magnetic Field Laboratory, HFIPS, Chinese Academy of Sciences, Hefei, Anhui 230031, China*
[2]*Science Island Branch of Graduate School, University of Science and Technology of China, Hefei 230026, China*
[3]*Photon Factory, Institute of Materials Structure Science, High Energy Accelerator Research Organization, Ibaraki 305-0801, Japan*

1 Introduction

Iridate system with the J_{eff}=1/2 pseudo-spin-half state represents as an excellent carrier for realizing exotic quantum phases such as Kitaev spin liquid, Mott insulator, and topological semimetal [1-3]. Iridates are also well known for the exceptionally strong magnetic anisotropy. One outstanding example is the strong easy-axis anisotropy in the bilayer square-lattice iridate $Sr_3Ir_2O_7$ [4]. On the contrary, the square-lattice single-layer iridate Sr_2IrO_4 only hosts a weak easy-plane anisotropy in the antiferromagnetic (AFM) ground state. As a result, the strong easy-axis anisotropy was ascribed to a dimensional effect, while the underlying mechanism may also relate to the intermediate electronic correlation. The dimensionality-driven spin flop transition was also observed in artificial lattices composed of $SrIrO_3$ and $SrTiO_3$. J. Matsuno et al. suggested that the $[(SrIrO_3)_1/(SrTiO_3)_1]$ superlattice also preserves an easy-plane magnetic anisotropy similar to Sr_2IrO_4 [5]. Later on, D. Meyers et al. confirmed that the $[(SrIrO_3)_2/(SrTiO_3)_1]$ superlattice hosts an easy-axis anisotropy similar to $Sr_3Ir_2O_7$. The authors also unveiled that the superlattice system is much closer to the spin-flop phase boundary than the bulk counterparts, which is beneficial for external modulation [6-8].

Aside from the dimensional effect, it was reported that lattice distortion plays a key role in the magnetic anisotropy of square-lattice iridates. Specifically, we recently designed and prepared a strongly distorted single-layer iridate superlattice $[(SrIrO_3)_1/(CaTiO_3)_1]$ superlattice [9]. In comparison to the non-distorted $[(SrIrO_3)_1/(SrTiO_3)_1]$ superlattice, the $[(SrIrO_3)_1/(CaTiO_3)_1]$ superlattice is characteristic of an exceptionally strong easy-plane anisotropy. Since similar lattice distortion can also be introduced into a bilayer system, a natural question arises of what the magnetic anisotropy of a square lattice iridate would be if there is coexistence of the dimensional effect and lattice distortion. Furthermore, while the dimensional effect is expected to be robust in a bilayer system, lattice distortion can be well controlled in a superlattice. It thus would be interesting to study the competition of easy-axis anisotropy and easy-plane anisotropy in bilayer square-lattice system. Through a delicate control of lattice distortion, the two terms may fully cancel out at a critical point. This work thus will offer an alternative route to pursue quantum phase transition in square-lattice magnetic systems, in complementing to the conventional routes by applying external pressure, magnetic field, etc.

2 Experiment

Experimentally, we prepared a series of $[(SrIrO_3)_2/(Sr_{1-n}Ca_nTiO_3)_1]$ (n = 0, 0.15, 0.25, 0.4, 0.5, 0.75, 1) superlattices with different chemical compositions, by using the RHEED-assisted pulsed laser deposition technique. We measured and analyzed the IrO_6 octahedra rotation and tilt of these superlattices.

3 Results and Discussion

Fig. 1(a) & (b) show the (0.5 0.5 1.5) and (0.5 1.5 1.5) Bragg peaks for all SLs. They represent out-of-plane (OOP) and in-plane (IP) out-of-phase rotations of IrO_6 octahedra, respectively [10-12]. As summarized in Fig. 1(c), the OOP rotation is almost n-independent from 0.5 to 1. When n < 0.5, where the in-phase rotation is unobservable, the variations of OOP and IP peaks exhibit opposing trends, suggesting that the OOP bond angle increases at the compensation of the IP bond angle. In this region, nonetheless, the modulation of octahedral rotation pattern is still nontrivial.

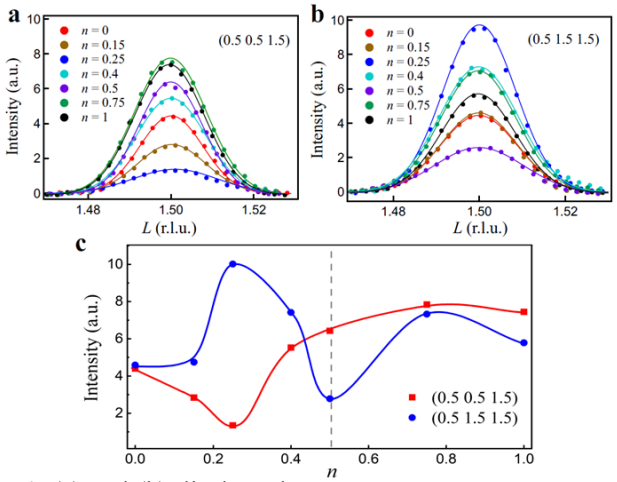

Fig. 1: (a) and (b) displays the room-temperature L-scans of $[(SrIrO_3)_2/(Sr_{1-n}Ca_nTiO_3)_1]$ (n = 0, 0.15, 0.25, 0.4, 0.5, 0.75, 1) SLs around the (0.5 0.5 1.5) and (0.5 1.5 1.5) reflections, respectively. (c) The extracted peak intensities of the (0.5 0.5 1.5), and (0.5 1.5 1.5) reflections at different n. The solid lines are guides for the eye.

While there is no in-phase octahedral rotation at $n = 0$, we observed a strong (1 0.5 1.5) reflection at $n = 1$ (Fig. 2(a)). As schematically shown in Fig. 2(b), the (1 0.5 1.5) reflection demonstrates that the in-phase rotation axis is along one of the IP axes. For simplicity, we hereafter denote the in-phase rotation axis as *a*-axis [10]. The peak intensity accounting for the emergent in-phase rotation is then summarized in Fig. 2(c), where the peak intensity is about 1/4 at $n = 0.75$, indicating that the *a*-axis anisotropy is reduced by half around $n = 0.75$.

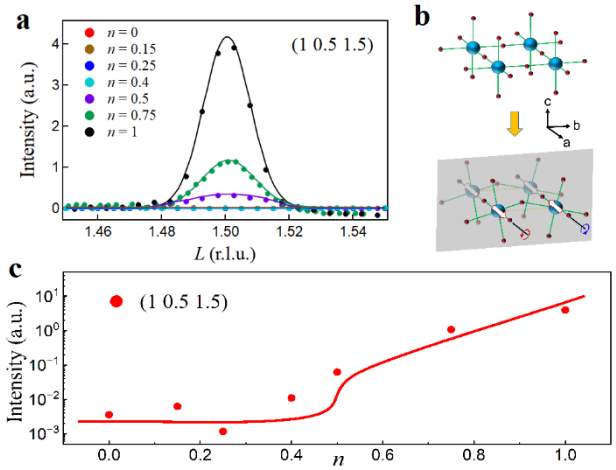

Fig. 2: (a) *L*-scan around the (1 0.5 1.5) reflection of different SLs. (b) Schematic diagram of the IP in-phase rotation. Gray plane is a mirror plane. The magnetic moments are denoted by open arrows. (c) The extracted peak intensities of the (1 0.5 1.5) reflection at different *n*. The solid lines are guides for the eye.

To determine the spin alignment, we performed REXS measurements on the $n = 1$ SL. As shown in Fig. 3, a well-defined magnetic reflection exhibiting a pronounced resonance effect at the Ir L_3-edge was identified at the half-integer position.

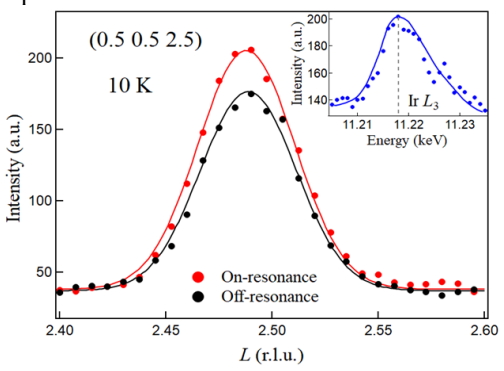

Fig. 3: On-resonance (red) and off-resonance (black) *L*-scans of the $n = 1$ SL across the (0.5 0.5 2.5) reflection at 10 K. The inset shows the energy profile of the Bragg reflection.

To exploit magnetic anisotropy, we performed magneto-transport measurements. As shown in Fig. 4(a), a large IP MR hysteresis was observed on the $n = 0$ SL. On the other hand, coercivity field in the $n = 1$ SL is negligible (Fig. 4(b)). This explicitly demonstrates that magnetic structures in the two SLs have distinct symmetries. This result is also consistent with the structural analysis (Fig. 2(c)).

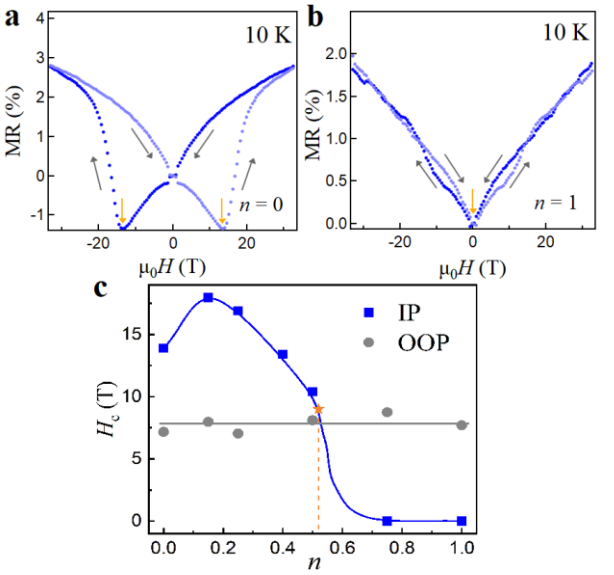

Fig. 4: (a) & (b) IP MR of the $n = 0$ and the $n = 1$ SLs at 10 K, respectively. Coercivity fields are denoted by brown arrows. (c) *n*–dependent coercivity fields of IP MR (blue square) and OOP MR (grey circle).

We then summarized the *n*-dependent coercivity field of IP MR in Fig. 4(c), from which one can qualitatively conclude that the *a*-axis anisotropy was reduced by half at $n \sim 0.5$. Nevertheless, within a single magnetic structure, *a*-axis and *c*-axis anisotropies should increase at the expense of the other. It is rational to expect that *a*-axis and *c*-axis anisotropies compete heavily around $n = 0.5$.

In conclusion, we modulated magnetic anisotropy in a bilayer pseudo-spin-half system through crystal design. The structure analysis indicates that the in-phase octahedral rotation that occurs during the transformation of the *c*-axis AFM at $n = 0$ SLs to the *a*-axis AFM structure at $n = 1$ of $[(SrIrO_3)_2/(Sr_{1-n}Ca_nTiO_3)_1]$ plays a crucial role. The investigation of magnetic coercivity reveals the dependence of the competition between different magnetic anisotropies due to *n*.

References

[1] J. Bertinshaw et al., *Annu. Rev. Conden. Ma. P.* **10**, 315 (2019).
[2] A. Lupascu et al., *Phys. Rev. Lett.* **112** (2014).
[3] J. G. Rau et al., *Annu. Rev. Conden. Ma. P.* **7**, 195 (2016).
[4] J. W. Kim et al., *Phys. Rev. Lett.* **109** (2012).
[5] J. Matsuno et al., *Phys. Rev. Lett.* **114** (2015).
[6] G. Cao et al., *Phys. Rev. B* **66** (2002).
[7] M. K. Crawford et al., *Phys. Rev. B* **49**, 9198 (1994).
[8] L. Hao et al., *Phys. Rev. Lett.* **119** (2017).
[9] J. Yang et al., *Phys. Rev. X* **12** (2022).
[10] M. Brahlek et al., *J. Appl. Phys.* **121**, 045303 (2017).
[11] A. M. Glazer, *Acta Cryst.* **A31**, 756 (1975).
[12] A. M. Glazer, *Acta Cryst.* **B28**, 3384 (1972).

* haolin@hmfl.ac.cn
https://doi.org/10.1016/j.newton.2026.100483 (Published)